



# PERTURBATIONS OF CLASSICAL ATOMS AND MOLECULES BY PERIODIC FIELDS

D. Richards

## ► To cite this version:

D. Richards. PERTURBATIONS OF CLASSICAL ATOMS AND MOLECULES BY PERIODIC FIELDS. Journal de Physique Colloques, 1982, 43 (C2), pp.C2-63-C2-80. 10.1051/jphyscol:1982206 . jpa-00221815

**HAL Id: jpa-00221815**

**<https://hal.science/jpa-00221815>**

Submitted on 4 Feb 2008

**HAL** is a multi-disciplinary open access archive for the deposit and dissemination of scientific research documents, whether they are published or not. The documents may come from teaching and research institutions in France or abroad, or from public or private research centers.

L'archive ouverte pluridisciplinaire **HAL**, est destinée au dépôt et à la diffusion de documents scientifiques de niveau recherche, publiés ou non, émanant des établissements d'enseignement et de recherche français ou étrangers, des laboratoires publics ou privés.

## PERTURBATIONS OF CLASSICAL ATOMS AND MOLECULES BY PERIODIC FIELDS

D. Richards

*Mathematics Faculty, The Open University, Walton Hall, Milton Keynes MK7 6AA, U.K.*

**Résumé.**— La théorie générale des systèmes classiques est brièvement passée en revue. L'effet de forces périodiques sur deux systèmes complètement distincts est étudié en détail.

On considère tout d'abord, un atome d'hydrogène classique dont on discute la réponse à des champs électriques périodiques de diverses fréquences et amplitudes. Quatre classes de comportement de l'électron sont alors possibles. Le second système considéré est celui de la rotation empêchée dans les molécules. On montre de quelle façon la perturbation périodique affecte les trajectoires résonnantes et comment le mouvement devient irrégulier lorsque des résonances sont trop proches.

**Abstract.** — The general theory of classical systems is briefly reviewed. The effect of periodic forces on two distinctly different systems is studied in detail.

First we consider a classical hydrogen atom in a periodic electric field and discuss the response of the atom to fields of different frequency and amplitude. The detailed motion of the electron is described and is categorised into one of four types.

Next we consider a different type of system characteristic of hindered rotations in molecules. It is shown how the periodic perturbation affects resonant trajectories, and how irregular motion is produced when resonances are too close.

1. **Introduction.** — Despite centuries of effort the behaviour of Hamiltonian systems is still not properly understood and is a subject of intense activity. Recent advances have been made by both analytic and computational studies, but the systems of direct interest to the atomic physics community are so complex that computations have so far been the most fruitful. However, these have necessarily been on specific systems and generalisations are not yet possible.

In the not too distant past the Hamiltonians relevant to atomic and molecular systems of interest were either integrable or so close to being integrable that perturbation methods were applicable. For these systems the motion is well understood and is the subject of the standard text books on analytic dynamics: we summarise this theory in section 2 and 3. But intense electro-magnetic fields produce systems described by Hamiltonians which are neither integrable nor close to integrable, and the motion of such systems is qualitatively different from that of integrable systems.

Here, I shall very briefly describe the effect of a periodic force acting on two distinctly different systems in order to illustrate how different systems behave. In section 4 we consider the ionisation of a hydrogen atom by a resonant electric field and in section 5 we consider a model system having some characteristics of a hindered rotator perturbed by a periodic force.

2. Conservative Integrable systems. - A Hamiltonian system of  $N$  degrees of freedom has a  $2N$ -dimensional phase space, points in which are labelled by a pair of conjugate variables  $(q, p) = (q_1, \dots, q_N, p_1, \dots, p_N)$ . A motion of the system is represented by a phase curve  $q_i(t), p_i(t), i = 1, \dots, N$ , usually parametrized by the time  $t$ ; for a bound conservative system with Hamiltonian  $H(q, p)$ , not depending explicitly upon the time, this curve usually fills a  $(2N-1)$ -dimensional region of phase space, as time tends to infinity. A system is said to be integrable if there exist  $N$  independent integrals  $F_i(q, p), i = 1, \dots, N$  satisfying the Poisson Bracket relations:

$$\{H, F_i\} = 0, \quad \{F_i, F_j\} = 0 \quad i, j = 1, 2, \dots, N. \quad (2.1)$$

The existence of these integrals means that each phase curve is confined to an  $N$ -dimensional surface in phase space given by the intersection of the  $N$   $(2N-1)$ -dimensional surfaces  $F_i(q, p) = \text{constant } i = 1, \dots, N$ .

Further, if the motion in phase space is bounded then it can be shown (see for example Arnold, 1978) that these surfaces are  $N$ -dimensional tori, so it is possible to choose a set of conjugate variables  $(\theta, I)$ , named angle-action variables, such that each torus is labelled uniquely by the action variables  $I$ , and the position on each torus is labelled uniquely by the values of the angle variables  $\theta_i \pmod{2\pi}, i = 1, \dots, N$ . The original variables  $(q, p)$  when expressed in terms of the angle-action variables will be multiply-periodic functions of  $\theta$ :

$$q(\underline{I}, \underline{\theta} + 2\pi \underline{s}) = q(\underline{I}, \underline{\theta})$$

where  $\underline{s}$  is an  $N$ -dimensional vector with integer components.

For a system of one degree of freedom the tori are simply closed one dimensional curves of constant energy, shown in figure (2.1) for the linear oscillator. For a system of two freedoms the four-dimensional phase space is filled with a set of two-dimensional tori, shown schematically in figure 2.2.

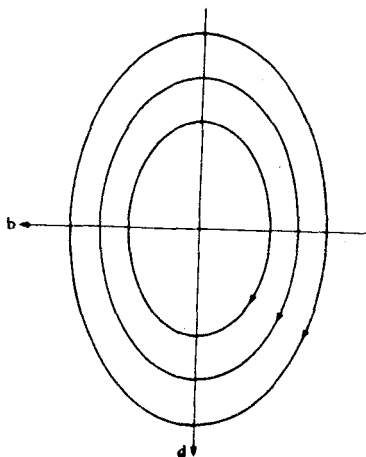
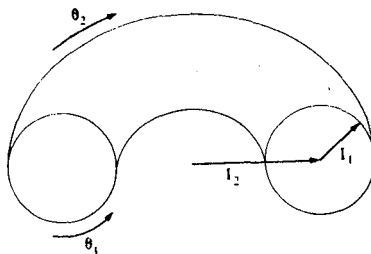


Figure 2.1

Sketch of the invariant tori of the linear oscillator with Hamiltonian  
 $H = p^2/2m + m\omega^2 q^2/2$



## 2.2 Sketch of the two-dimensional torus for a system of two degrees of freedom showing the coordinates $(\theta_1, \theta_2, I_1, I_2)$

Because the motion lies on a torus, the actions  $\underline{I}$  are constants and the Hamiltonian in angle-action representation must be independent of  $\underline{\theta}$ ,

$$H(\underline{q}(\underline{\theta}, \underline{I}), \underline{p}(\underline{\theta}, \underline{I})) = K(\underline{I}), \quad (2.2)$$

and from Hamilton's equation the angle variables vary linearly with time

$$\dot{\theta}_k = \frac{\partial K}{\partial I_k} = \omega_k(\underline{I}) \quad \text{or} \quad \theta_k = \omega_k(\underline{I})t + \delta_k, \quad k = 1, \dots, N. \quad (2.3)$$

Here the  $\omega_k(\underline{I})$  is the frequency of the motion around the  $k$ 'th cycle of the torus. It is important to notice that these frequencies almost always depend upon the actions: that is, with each torus is associated a different set of frequencies.

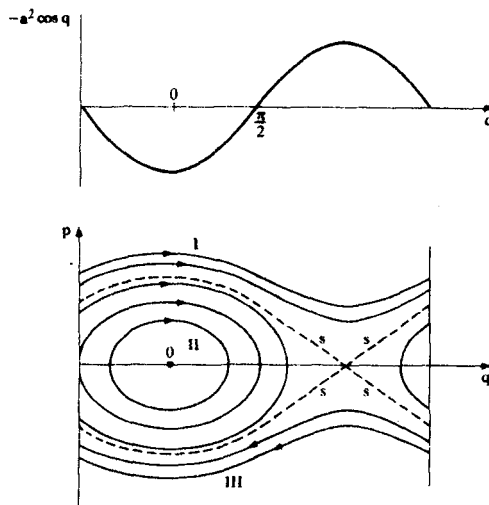
The last observation has a simple but, as we shall see, crucial consequence, easiest to describe for system of 2 freedoms, but not restricted to these. The ratio of frequencies  $R(\underline{I}) = \omega_1(\underline{I})/\omega_2(\underline{I})$  for some values of  $\underline{I}$  will be rational,  $R = s_1/s_2$ , and for other values will be irrational these are called proper tori. In the former case the motion is periodic, with period  $2\pi s_1/\omega_1$  and the phase curve does not fill the torus: in the latter case the phase curve approaches arbitrarily close to any given point on the torus. This is an important distinction between the two types of tori. Since any real number can be approximated arbitrarily accurately by a rational number any proper torus is arbitrarily close to a torus with rational  $R$  even though the probability of picking out a "rational" torus at random is zero.

The best known examples of integrable systems are those with Hamiltonians which are separable in some coordinate system  $(Q, P)$ . Such Hamiltonians can be written as a sum of  $N$  Hamiltonians all having one degree of freedom, so each sub-Hamiltonian is separately conserved. Examples of such systems are central forces, Stark effect on hydrogen atoms, Linear Zeeman effect on Hydrogen atoms, two fixed centres of Coulomb force, a heavy symmetric top rotating about a fixed point, an asymmetric top rotating about its centre of gravity.

The geometric picture given above is deceptively simple and is often complicated by features present in the simplest of systems. An important example is given by the Hamiltonian,

$$H(q, p) = \frac{1}{2A} p^2 - a^2 \cos q, \quad (A > 0) \quad (2.4)$$

which describes the motion of a vertical pendulum, the hindered rotations of one part of a molecule with respect to the remainder (see for example Townes and Schawlow 1975) and is also an approximation valid in small regions by phase space to the Hamiltonian of more complicated systems. It is in this context that we shall meet it again in section 5. For the present discussion it is easiest to visualise as the motion of a vertical pendulum with  $q$  the angle between the pendulum and the downward vertical.



2.3 Sketch of the potential and phase curves for the Hamiltonian (2.4). The dashed curve is the separatrix,  $s$ ; the significance of regions I, II and III is described in the text.

There are then three types of motion. First the small oscillations about  $q = 0$ , and second the rotational motion in which  $q(t)$  is always increasing or always decreasing. These types of motion are seen in the phase curves of the Hamiltonian shown in figure 2.3. The closed curves centred on 0, region II, correspond to small oscillations: if the energy,  $W$ , of the system lies in the range  $-a^2 < W < a^2$  the motion is of this type. At higher energies  $W > a^2$ , regions I and III, the phase curves are not closed but are periodic with period  $2\pi$ , as a consequence of the periodicity of configuration space. Region I represents anti-clockwise and region III clockwise motion.

The third type of motion separates these two periodic motions and is represented by the dashed curve  $s$  in figure 2.3. We call  $s$  the separatrix and it represents motion with energy  $E = a^2$  which is just sufficient for the pendulum asymptotically to reach the upward vertical: this is clearly an unstable motion and it is not periodic.

In either of regions I, II or III angle-action variables can be found, equation 5.2, but the angle-action variables of one region are unrelated to those of the other regions.

Thus even for this simple system the phase space is divided into distinct regions each with different types of motion so that the canonical transformation to angle-action representation is discontinuous across the separatrix. A perturbation may produce an arbitrarily large number of separatrices in a bounded region of phase space, see section 5, with the possible consequences that the differentiable transformation to angle-action variables ceases to exist.

3. Perturbations of Integrable systems. - Most systems are not integrable in the sense described above and the general features of their behaviour are not generally understood. In these circumstances it is natural to consider a slightly perturbed integrable system,

$$H(q, p) = H_0(q, p) + \epsilon H_1(q, p) \quad (3.1)$$

where  $H_0$  is integrable and the perturbation  $\epsilon H_1$  is "small". Then if the perturbation is small enough there is an existence theorem due to Kolmogorov, Arnold and Moser (see for example Arnold 1963, Arnold 1978), the KAM Theorem, which guarantees that most of the original proper tori of  $H_0$  are only slightly distorted by the perturbation. In practice the bounds on  $\epsilon H_1$  imposed by this theorem mean that it is not applicable in most interesting physical circumstances, but numerical evidence suggests that the result holds for rather larger perturbations, which are of physical relevance.

The KAM theorem is silent upon the fate of tori with rational frequency ratios, and, as we shall see in section 5, it is these that appear to cause many of the difficulties. Briefly, on these tori the perturbation creates a separatrix dividing the original torus into regions having different types of motion, exactly like those occurring with the Hamiltonian (2.4). As there are an infinity of such rational tori, and as each proper tori is arbitrarily close to a rational torus the ensuing structure of phase space becomes very complex. For small perturbations this complexity is contained, and most of phase space is filled with proper tori, as the perturbation increases the effect of the rational tori becomes more significant and eventually most proper tori disappear. This will be demonstrated explicitly in section 5.

So far all discussion has concerned conservative systems. In the next two sections we shall deal with systems for which the perturbation is periodic in time:

$$\begin{aligned} H(q, p, t) &= H_0(q, p) + \epsilon H_1(q, p, t) \\ H(q, p, t+T) &= H(q, p, t). \end{aligned} \quad (3.2)$$

By introducing new conjugate variables  $q_{N+1} = t/T$  and  $p_{N+1}$  and the new Hamiltonian

$$K = p_{N+1} + H(q, p, q_{N+1}) \quad (3.3)$$

it is easily seen that the above remarks apply equally well to this periodically-forced conservative system.

4. Hydrogen atom in an oscillating field. - The motion of an electron in a combined Coulomb and uniform periodic electric field is very complicated and little understood. But as both experiments (Bayfield and Koch 1974, also Bayfield 1979) and numerical computations (Leopolod and Percival 1979, Mostowski and Sanchez-Mondragon 1979, Jones et al 1980) have been performed on this system, with reasonable agreement, it affords a useful introductory example.

The model Hamiltonian for the system is

$$H = H_c(\underline{r}, \underline{p}) + zF A(t) \cos \omega t \quad (4.1)$$

where

$$H_c = \frac{p^2}{2} - 1/r$$

is the unperturbed hydrogen atom Hamiltonian;  $A(t)$  is a switching function which

adiabatically switches the oscillating field on and off (see Leopold and Percival 1979), introduced in order to approximate experimental conditions. Here we need only note that  $A(t)$  increases slowly from zero to unity over many forcing periods, remains at unity for many periods then decays slowly to zero (see figure 1 Leopold and Percival 1979).

It is useful to define units of force and frequency appropriate to the unperturbed motion. The unit of frequency is that of the unperturbed electron motion:

$$\text{frequency: } \omega_{\text{at}} = (\text{atomic unit})/n^3 \quad (4.2)$$

where  $n$  is the initial principal quantum number. Note that  $\omega_{\text{at}}$  is approximately the frequency of transition between adjacent states:

$$\omega_{\text{at}} \approx (E_{n+1} - E_n)/\hbar \quad (4.3)$$

$E_n$  being the quantal energy level. The unit of force is taken to be the mean Coulomb force:

$$\text{force: } F_{\text{at}} = (\text{atomic unit})/n^4. \quad (4.4)$$

Thus we can define two dimensionless parameters characterising the interaction

$$\tilde{\omega} = \omega/\omega_{\text{at}}, \quad \tilde{F} = F/F_{\text{at}}. \quad (4.5)$$

The scale of  $\tilde{F}$  is set by the smallest field needed to produce any ionization in the static limit ( $\tilde{\omega} = 0$ ). Banks and Leopold (1978) find this to be  $\tilde{F} = 0.13$ . For time-varying fields ionization can occur at much lower levels of  $\tilde{F}$ , see figure 4.1.

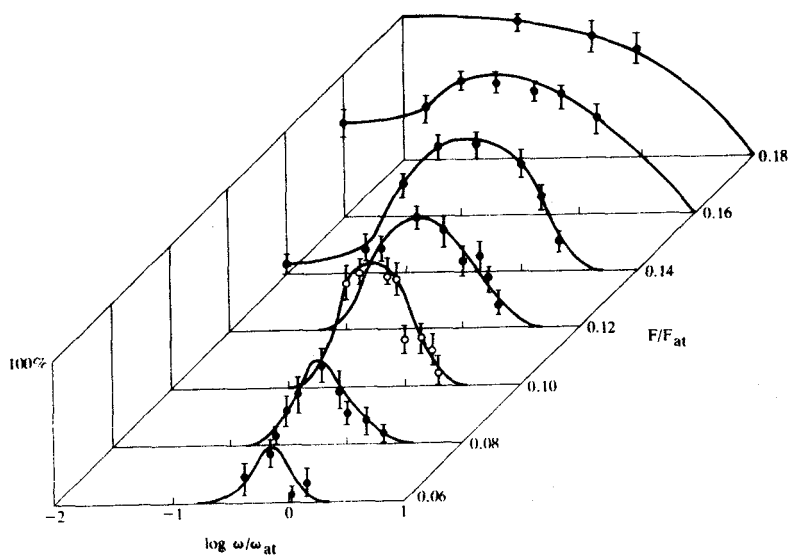
The significant values of  $\tilde{\omega}$  will be seen to be  $\tilde{\omega} \approx 1$ . For small  $\tilde{\omega}$  the field variation is adiabatic with respect to the electron motion and affects the atom as if it were a static field. For large  $\tilde{\omega}$  the field oscillates many times during one electron period producing a zero net effect.

The probabilities of ionization for various  $\tilde{\omega}$  and  $\tilde{F}$  are shown in figure (4.1). It is seen that for small  $\tilde{F}$  the most dramatic effects are for  $\tilde{\omega} \approx 0.8$  and that as  $\tilde{F}$  increases the significant range of  $\tilde{\omega}$  increases. A similar effect is seen in the calculations of Martin and Wyatt (1982) and of Walker and Preston (1977).

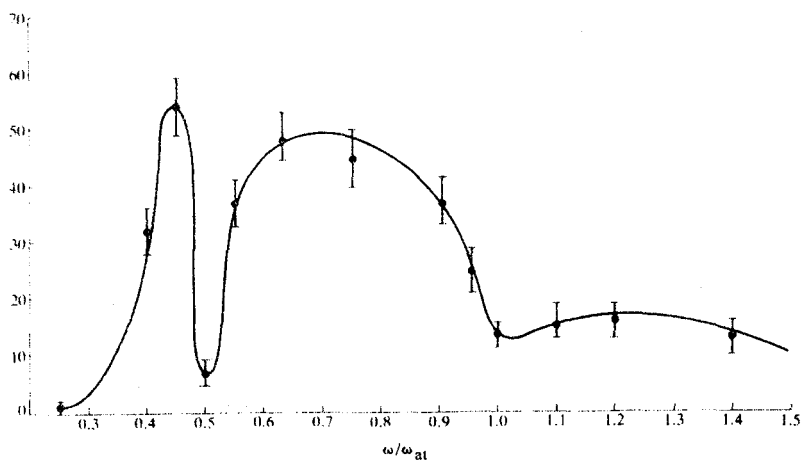
This apparent simplicity masks the complexity of the mechanism producing ionization. A more detailed study of the frequency response is shown in figure (4.2): here it is seen that the ionization probability is a fairly complicated function of  $\tilde{\omega}$ , and that it has a sharp dip at about  $\tilde{\omega} \approx 0.5$ . The reasons for this are not known.

Further analysis of the trajectories shows that each classical trajectory can be classified into one of four classes which are

- C1 Trajectories on tori, which probably never ionize;
- C2 Trajectories that ionise rapidly;
- C3 Trajectories passing through one or more extremely highly excited (EHE) states with relatively sudden transitions between them before ionizing; and
- C4 Trajectories which pass through a sequence of EHE states but do not ionise during the time of computation. These would probably ionise eventually.



4.1 Three dimensional plot showing the percentage ionization, vertical scale, as a function of both frequency and amplitude. The Monte-Carlo method used to generate these results is described by Leopold and Percival 1979: it is this method which produces the statistical errors shown by the error bars.



4.2

Percentage ionization as a function of  $\omega/\omega_{at}$  for  $F = 0.08 F_{at}$



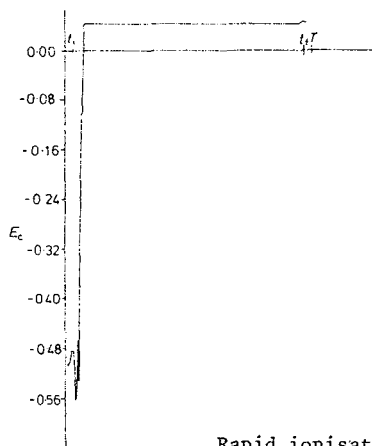
The differences between these types of trajectories are clearly seen in the time dependence of the compensated energy  $E_c(t)$ . This compensated energy allows for the oscillation produced by the field: in the absence of the Coulomb field the velocity of the electron is

$$\underline{v} = \underline{v}_0 - \frac{F}{m\omega} \underline{z} \sin \omega t, \quad (4.6)$$

$\underline{v}_0$  being a constant vector, so the compensated energy is defined as

$$E_c(t) = \frac{m}{2} [v_x^2 + v_y^2 + (v_z + \frac{F}{m\omega} \sin \omega t)^2] - \frac{1}{r}. \quad (4.7)$$

When the Coulomb field is weak  $E_c(t)$  is almost constant and is approximately the mean kinetic energy of the electron over one oscillation. When  $E_c > 0$  ionization is assumed to have occurred.



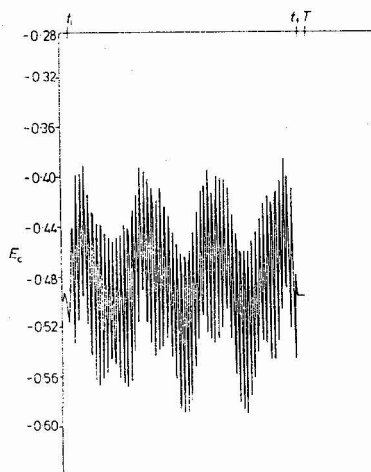
Rapid ionisation (C2)

#### 4.3 $E_c$ against time for an ionised trajectory.

In figure 4.3 is shown the compensated energy for a C2 type trajectory. In figure 4.4 a C1 type of trajectory is given. Here we see that  $E_c$  oscillates around the initial energy. When the field is turned off adiabatically,  $E_c$  becomes the actual total energy which is nearly the same as the initial energy. This is an example of an invariant torus, which does not ionise. In figure 4.5 before  $E_c$  becomes positive and constant (ionization) it is for some time negative and  $E_c$  constant. When the positions and velocities are checked we find that the electron moves slowly in a very large Kepler ellipse, with wobbles due to the external field. The period of revolution is proportional to

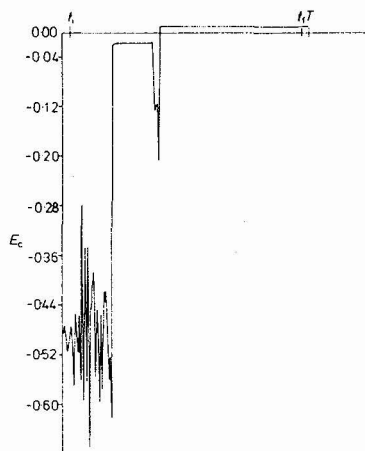
$$E_c^{-3/2}.$$

The electron is in an extremely highly excited (EHE) state.



Invariant torus (C1)

4.4  $E_c$  against time for an invariant torus type of trajectory.



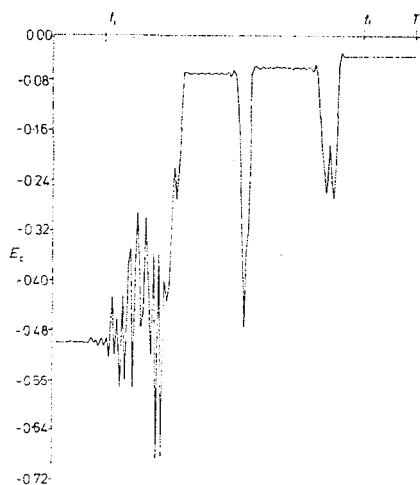
Ionisation via EHE (C3)

4.5  $E_c$  against time for a trajectory which ionises via some stable EHE states.

If the field is turned off adiabatically during the time the electron is in an EHE state like in figure 4.6 the total energy remains negative and constant resulting in a final EHE state.

The behaviour shown in these graphs can be understood qualitatively. In the absence of a field the electron moves in an elliptical orbit with characteristic binding energy and frequency. In the absence of the proton the electron moves uniformly in the mean but imposed on this uniform motion is a sinusoidal oscillation (equation 4.6) with characteristic mean kinetic energy and frequency.

In neither case does the electron lose or gain energy in the mean. But when both proton and field act together the interesting things happen, and the electron can gain or, more rarely, lose energy. The particular type of phenomena which occur depend on the frequency ratio and energy ratio for the proton and field.



Final EHE state (C4)

4.6  $E_c$  against time for a trajectory in a final EHE state.

As discussed above, if the field frequency is too small or too large little of interest happens. But for  $\omega$  near unity more interesting effects occur. In the first type (C1, figure 4.4) the trajectory appears to be an invariant torus in phase space and on this trajectory there is no effective energy transfer; the motion is made up of sinusoidal components and is said to be multiply periodic. The electron never goes very much further from the proton than when it was in the original elliptical orbit, in the absence of the field.

In the second type (C2, figure 4.3) the oscillating field and the proton work together in the early stages of the full strength field, and after relatively few oscillations the electron is ionized. These are probably the initially more eccentric orbits.

In the more interesting third and fourth types the electron gains energy in the early stages as in the second type, but not enough to ionize. It moves away from the proton into an elliptical orbit upon which are superimposed the sinusoidal oscillations of the field. The orbit is eccentric, often highly eccentric, with its perihelion at a similar distance from the nucleus to  $a$ , the initial and semi-major axis, and its aphelion many times further away. The calculations show that compensated energy is very stable in the outer ranges of these orbits, near the aphelion, and indeed anywhere on the orbit which is significantly further from the proton than  $a$ . The sudden changes in energy illustrated in figures 4.4, 4.5, 4.6 takes place when the electron is near the perihelion. The time between these sudden changes is approximately proportional to

$$E_c^{-3.2}.$$

This is what would be expected from our interpretation. Notice that the weaker the binding, the more stable the atom is in the presence of the oscillating field.

Each time the electron approaches perihelion it changes its orbit. It may occasionally ionize, or it may be excited to an even more highly excited state, or, more rarely, to a less excited state. As time goes on, those atoms which have not ionized, and whose electron trajectories are not on invariant tori, reach higher and higher excited states or EHE states.

The EHE orbits are remarkably stable in the presence of the field. They have frequencies which are very much lower than the field frequency, the opposite of adiabatic, so the orbit has very many sinusoidal oscillations imposed on its basic elliptical shape. Their lifetime is given by the

$$E_c^{-3/2}$$

law, so we find that atoms can be relatively stable in the presence of oscillating electric fields, even if the magnitude of those fields is many times the magnitude of the static field required to produce Stark ionization.

The third and fourth types of orbit are distinguished only by the fact that for the third type ionization does eventually take place during the period considered whereas in the fourth type it does not. It is probable that any orbit of the fourth type would eventually ionize.

This qualitative description of the trajectories shown in figures 4.3 to 4.6 provides a clue to the features required in any approximate analytic theory. At present there is no simple theory which will satisfactorily predict the results produced by these numerical calculations. For this reason we turn to a simple system in order to understand better the complexities of the dynamics.

5. A periodically forced system of one degree of freedom. - A simpler system which has received some attention (Rechester and Stix 1979, Escande and Doveil 1981, see also Chirikov 1979 and references therein) is the Hamiltonian (2.4) perturbed by a potential periodic in space and time:

$$H(q,p,t) = \frac{1}{2} p^2 - \cos q + \varepsilon \cos(\lambda q - \Omega t) \quad (5.1)$$

which may be taken to represent a hindered rotator or a vertical pendulum acted upon by a time-varying field.

The phase curves of the unperturbed motion,  $\varepsilon = 0$ , are shown in figure 2.3. In order to analyse the effects of the perturbation it is easiest to work with the angle-action variables of the unperturbed system:

$$\begin{aligned} I &= \frac{2}{\pi} \int_0^{q_1} dq \sqrt{2(W - \cos q)} \quad \cos q_1 = W, \\ &= \frac{8}{\pi} k(1 - k^2) \frac{dK}{dk} \quad k^2 = (1 + W)/2, \quad |W| < 1 \end{aligned} \quad (5.2)$$

$$\begin{aligned} I &= \frac{1}{2\pi} \int_{-\pi}^{\pi} dq \sqrt{2(W - \cos q)} \\ &= \frac{4}{\pi k_1} E(k_1) \quad k_1^2 = 2/(W - 1), \quad |W| > 1. \end{aligned} \quad (5.3)$$

where  $W$  is the energy and  $K(k)$  and  $E(k)$  are complete elliptic integrals and of the first and second kind respectively. The relation between the energy and action and frequency and action are shown graphically in figure 5.1. The most important aspect of the frequency relation is the rapid decrease to zero as  $W \rightarrow 1$ : more precisely

$$\begin{aligned}\omega &= \pi/2K(k) \\ &\cong \pi/\ln\left(\frac{32}{1-W}\right), \quad W \lesssim 1.\end{aligned}\tag{5.4}$$

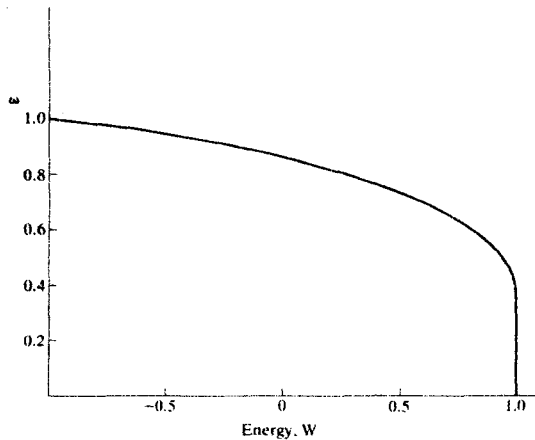


Fig. 5.1

The unperturbed motion is particularly easy to understand because the phase space is two dimensional and the phase curves easy to draw. The perturbation spoils this simplicity by introducing another dimension, time, so we need an alternative method of representing the solution. One of the most convenient techniques is to look at  $(q(t), p(t))$  at regular intervals equal to the period of the forcing term, that is to view the system using a stroboscope of the same frequency as the forcing term. Then we see a set of points

$$(q_s, p_s) = (q(t_s), p(t_s)) \quad t_s = 2\pi s/\Omega, \quad s = 0, 1, \dots\tag{5.5}$$

which can be plotted as a sequence in the two dimensional  $(q, p)$  phase space.

Clearly the phase point  $(q_{s+1}, p_{s+1})$  is uniquely determined by the previous phase point  $(q_s, p_s)$ :

$$(q_{s+1}, p_{s+1}) = \underline{F}(q_s, p_s).\tag{5.6}$$

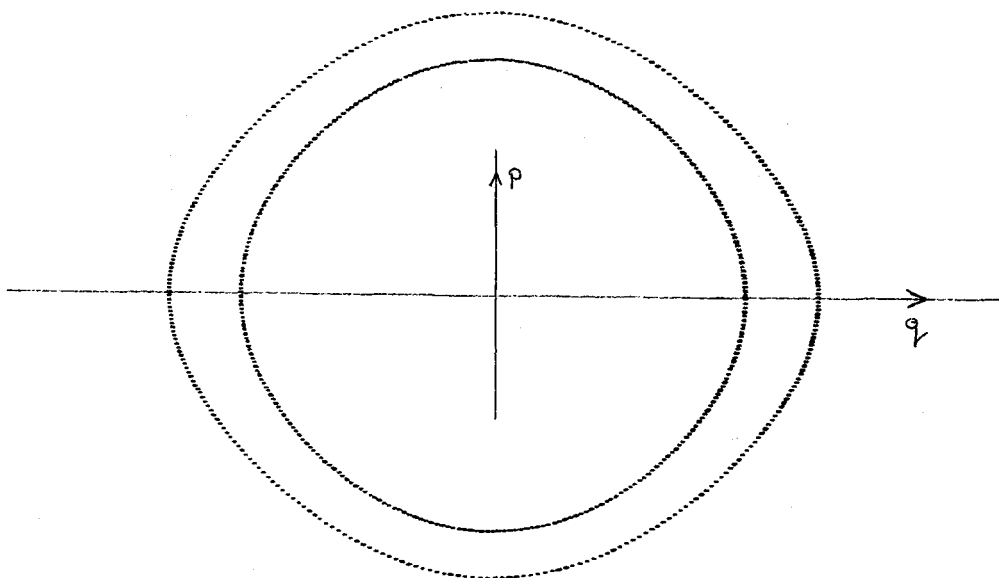
It can also be shown that because the original system is Hamiltonian the mapping (5.6) is area-preserving.

If this technique is applied to the unperturbed problem each sequence with a given energy  $W$  lies on the appropriate phase curve of figure 2.3. If the ratio  $\omega(W)/\Omega$  is irrational the sequence of points will eventually fill the phase curve, but if  $\omega/\Omega$  is rational,  $r/s$  say, then after  $s$  periods the sequence will repeat itself, that is the mapping is periodic with period  $s$ :

$$(q_s, p_s) = (q_0, p_0) \quad (\omega/\Omega = r/s).\tag{5.7}$$

The perturbation to the original Hamiltonian causes a perturbation to the mapping (5.6), and no matter how small this perturbation is its effect is very complicated.

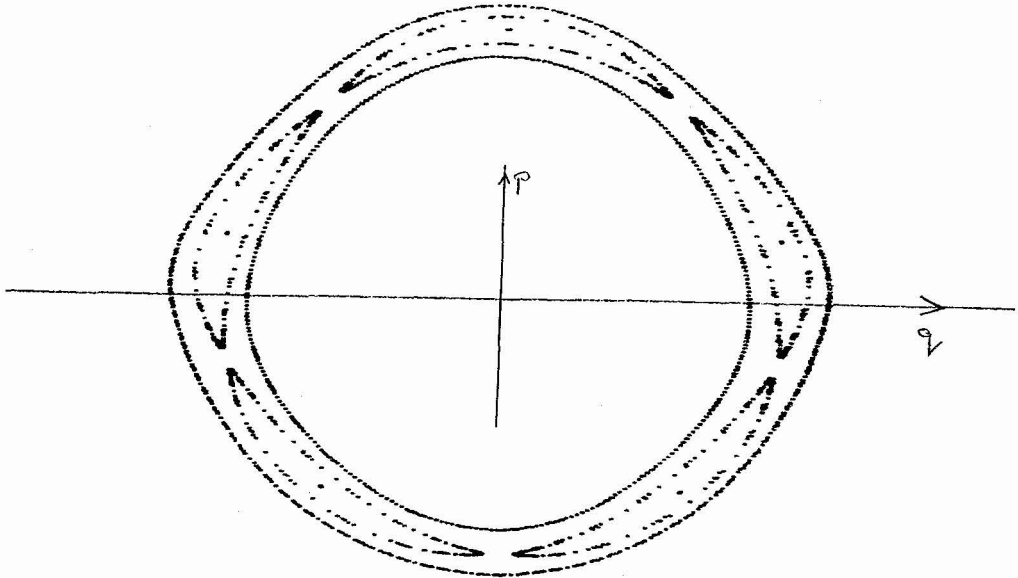
Consider a perturbation of the trajectory for which  $\omega/\Omega = r/s$ , so that there are  $s$  unperturbed fixed points  $(q_i, p_i)$ ,  $i = 0, 1, \dots, s-1$ , then a general theorem (Arnold and Avez 1968 section 20) shows that for sufficiently small perturbations, and some  $k$ ,  $2ks$  fixed points are produced and that half these are stable and half unstable.



5.2 Stroboscopic plot of the unperturbed system,  $\epsilon = 0$ . Three trajectories are shown; the five distinct dots is the trajectory with  $\omega = 4/5$ : these are surrounded by closed curves of larger and smaller frequency (smaller and larger energy).

This behaviour is seen clearly in figures 5.2 and 5.3. The first of these figures shows the unperturbed trajectory with  $\omega = 4/5$  and two neighbouring trajectories: the second shows the effect of the perturbation on these trajectories, and here the five stable fixed points are clearly seen; remember that all of these points are obtained from a single trajectory. Surrounding these fixed points are small "islands"; only one trajectory producing the islands is shown in figure 5.3. The trajectories forming these islands behave qualitatively differently from any of the unperturbed trajectories. On the other hand the inner and outer trajectories shown in figure 5.3 are qualitatively similar to the unperturbed trajectories shown in figure 5.2.

In figure 5.3 five stable fixed points are shown and the five unstable fixed points are not shown although their approximate position is clear. Neither is the separatrix passing through these unstable fixed points shown. When these features are included the local structure of the phase curves looks very similar to that of the unperturbed pendulum figure 2.3.



5.3 Diagram showing the effects of a small perturbation,  $\epsilon = 0.1$ , on trajectories near those of figure 5.2. A total of four trajectories is shown; one, producing the five dots, has a perturbed frequency of  $4/5$ , surrounding these dots are five islands produced by a neighbouring trajectory. Surrounding these islands are two trajectories similar to those of the unperturbed trajectories of figure 5.2.

Now consider a more detailed analysis of the perturbation. In angle-action representation the perturbation may be written as the Fourier series

$$\cos(\lambda q - \Omega t) = \sum_n V_n(I) \cos(n\theta - \Omega t + \alpha_n) \quad (5.8)$$

$$V_n(I) e^{i\alpha_n} = \frac{1}{2\pi} \int_{-\pi}^{\pi} d\theta \exp i(\lambda q(\theta) - n\theta) \quad (5.9)$$

so that the full Hamiltonian is

$$H = H_0(I) + \epsilon \sum_n V_n(I) \cos(n\theta - \Omega t + \alpha_n). \quad (5.10)$$

Then the equations of motion are

$$\dot{\theta} = \omega(I) + \epsilon \sum_n \frac{dV_n}{dI} \cos(n\theta - \Omega t + \alpha_n) \quad (5.11)$$

$$\dot{I} = \epsilon \sum_n n V_n(I) \sin(n\theta - \Omega t + \alpha_n).$$

A straightforward perturbative solution is

$$\theta = \omega(I_0)t + \theta_0 + \sum_n \frac{dV_n}{dI_0} \frac{\sin((n\omega(I_0) - \Omega)t + \alpha_n + n\theta_0)}{n\omega(I_0) - \Omega} \quad (5.12)$$

$$I = I_0 - \varepsilon \sum_n nV_n(I_0) \frac{\cos((n\omega(I_0) - \Omega)t + \alpha_n + n\theta_0)}{n\omega(I_0) - \Omega} \quad (5.13)$$

where  $(\theta_0, I_0)$  are the initial values of  $(\theta, I)$ . Clearly if  $|n\omega(I_0) - \Omega|$  is not small for any  $n$  this simple solution is reasonably accurate and we should expect the phase curves to be only slightly perturbed. But for those phase curves for which  $n\omega(I_0) \approx \Omega$  for some  $n$  this expansion is invalid. Note that in this case the unperturbed mapping is periodic with period  $n$ .

Now concentrate on the perturbation to an unperturbed motion with action  $I \approx I_m$  where

$$m \omega(I_m) = \Omega. \quad (5.14)$$

Then if  $I_m$  is not too close to  $I_{m+1}$  all terms in the sum of equation (5.10) other than  $n = m$  will be rapidly varying and, as in the Rotating-wave approximation (see for example Knight and Milonni 1980), may be ignored to give

$$H \approx K(\theta, I, t) = H_0(I) + \varepsilon V_m(I) \cos(m\theta - \Omega t + \alpha_m). \quad (5.15)$$

This time dependent Hamiltonian can be converted to a time independent Hamiltonian by using the canonical transformation

$$J = I \quad \phi = \theta - \frac{\Omega t}{m} + \frac{\alpha_m}{m} \quad (5.16)$$

which gives

$$K(\phi, J) = H_0(J) - \frac{J\Omega}{m} + \varepsilon V_m(J) \cos m\phi \quad (5.17)$$

But since  $I$  is close to  $I_m$  we put

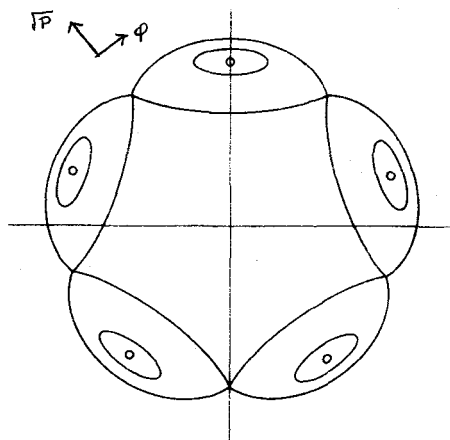
$$J = I_m + P \quad (5.18)$$

and assume  $P$  small. Then to within an irrelevant additive constant

$$K(\phi, P) = \frac{1}{2} \omega'(I_m) P^2 + \varepsilon V_m(I_m) \cos m\phi. \quad (5.19)$$

The justification for ignoring higher terms in this expansion will become clear soon.





5.4 Sketch of the phase curves for the Hamiltonian (5.19). Here  $\sqrt{P}$  and  $Q$  are interpreted as polar coordinates.

The Hamiltonian (5.19) is similar to that of the vertical pendulum, equation 2.4, the main difference being that  $\theta$  is replaced by  $m\phi$ , so that for  $\phi \in (0, 2\pi)$  there are  $2m$  fixed points, at  $\phi = r\pi/m$   $r = 0, 1, \dots, (2m-1)$ ,  $p = 0$ : half of these are stable around which  $(\phi, P)$  executes small oscillations. In between these are the  $m$  unstable fixed points joined by separatrixes. Outside the separatrixes the motion is similar to the unperturbed motion. In the case  $m = 5$  this is shown schematically in figure 5.4 in which  $\sqrt{P}$  and  $\phi$  are treated as polar coordinates. The maximum distance separating the separatrixes is

$$\Delta P = 4\sqrt{\epsilon} \left| \frac{V_m}{\omega_0^2} \right|. \quad (5.20)$$

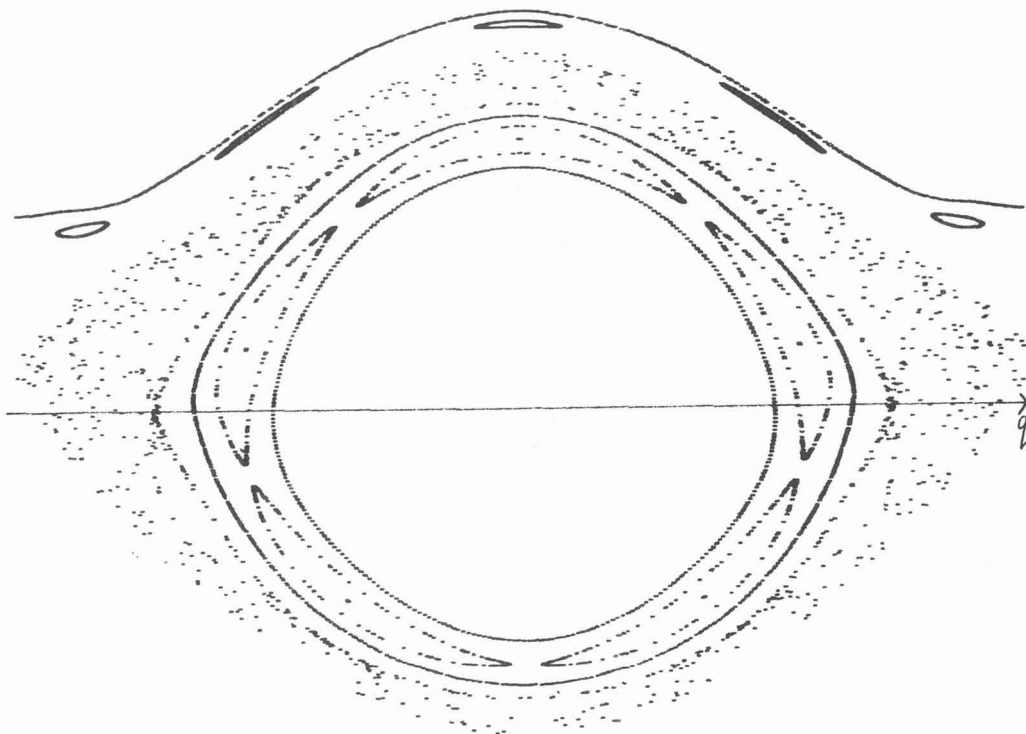
The motion in the original  $(\theta, I)$  representation is easily obtained from figure (5.4) by noting that (5.16) is equivalent to transformation to a reference frame rotating with angular speed  $\Omega/m$ . Thus our stroboscope will pick out the values of  $\theta$ ,

$$\theta_s = \phi(t_s) - \frac{2\pi s}{m} \quad t_s = 2\pi s / \Omega. \quad (5.21)$$

That is, each successive time that the system is lit up we see motion around adjacent fixed points in the  $(\phi, P)$  representation.

This quite simple analysis satisfactorily explains the behaviour shown in figure 5.3.

In figure 5.5 is shown the effect of the perturbation of a librating trajectory at higher energies. In this figure seven trajectories are shown: the inner four are the same as shown in figure 5.4. The outer curve corresponds to an unperturbed rotational motion, and the islands underneath it belong to a set of fixed points in the rotational region. The unstructured sequence of dots all belong to a single trajectory: this sequence does not lie on any simple curve and clearly the trajectory producing this sequence is of a different kind to any previously encountered. It is named an irregular trajectory (Percival 1973).



5.5 Stroboscopic plot showing an irregular trajectory of the Hamiltonian (5.1)

For this irregular trajectory the previous analysis is invalid as the assumption that neighbouring resonant terms do not interfere is invalid. From figure 5.1 it can be seen that as  $m$  increases the difference  $I_{m+1} - I_m$  decreases rapidly. If

$$I_{m+1} - I_m \approx \text{separatrix width} = 2\sqrt{\epsilon} \left| V_m / \omega_0' \right| \quad (5.22)$$

then the Hamiltonian (5.15) is no longer a reasonable approximation to the system. Of course as  $m$  increases  $|V_m|$  decreases, but the numerical work of Rechster and Stix (1979) shows that at  $m \approx 6$  equality (5.22) holds. It is the overlapping of these resonant terms which causes the break-up of the tori (see for example Chirikov 1979) and the condition (5.22) gives an approximate criterion for the destruction of the invariant tori.

When condition (5.22) is satisfied the full Hamiltonian may be approximated satisfactorily by including both the  $n = m$  and  $n = m + 1$  resonant tori. This Hamiltonian is not integrable, but the more sophisticated renormalisation methods of Escande and Doveil (1981) may be used to give a more accurate criterion of the onset of chaos.

#### Acknowledgement

I thank Professor I. C. Percival for useful discussion during the preparation of this article and for his, Drs Jones and Leopold's permission to publish the figures of section 4.

References

- ARNOLD V.I., Russian Math Surveys 18 (1963) 85-191
- ARNOLD V.I., Mathematical methods of classical mechanics (1978) (Springer-Verlag)
- ARNOLD V.I. and AVEZ A., Ergodic Problems of Classical Mechanics (1968) (Benjamin)
- BANKS D. and LEOPOLD J.G., J. Phys. B 11 (1978) 37-46
- BAYFIELD J.E., Phys. Rep. 51 (1979) 317-391
- BAYFIELD J.E. and KOCH P.M., Phys. Rev. Lett. 33 (1974) 258-61
- CHIRIKOV B.V., Phys. Rep. 52 (1979) 263-379
- ESCANDE D.F. and DOVEIL F., Phys. Lett. 83A (1982) 307-10
- JONES D.A., LEOPOLD J.G. and PERCIVAL I.C., J. Phys B 13 (1980) 31-40
- KNIGHT P.L. and MILONNI P.W., Phys. Rep 66 (1980) 21-107
- LEOPOLD J.G. and PERCIVAL I.C., J. Phys B 12 (1979) 709-21
- MARTIN D.L. and WYATT R.E., Chem.Phys 64 (1982) 203-220
- MOSTOWSKI J. and SANCHEZ-MONDRAGON J.J., Opt. Comm 29 (1979) 293-6
- PERCIVAL I.C., J. Phys. B, 6 (1973) L229-32
- RECHESTER A.B. and STIX T.H., Phys. Rev. A19 (1979) 1656-65
- TOWNES C.H. and SCHAWLOW A.L., Microwave Spectroscopy (1975) (Dover)
- WALKER R.B. and PRESTON R.K., J. Chem . Phys. 67 (1977) 2017-28